Mathematical & Computational Applications, Vol. 7, No. 2, pp. 171-179, 2002

EFFECT OF PLATE SPACING OF IMPINGEMENT AIR JET ON FLOW AND HEAT TRANSFER CHARACTERISTICS

Mehmet Kopaç
Department of Mechanical Engineering
Zonguldak Karaelmas University 67100 Zonguldak, Turkey

Abstract-In this paper the flow and heat transfer characteristics in the turbulent confinement impinging air jet have been numerically analyzed. Two-equation turbulence model, κ-ε, have been used. Mass, momentum, energy, turbulent kinetic energy and turbulent kinetic energy dissipation rate equations were solved by the PHOENICS package program. Velocity, turbulent kinetic energy, turbulent kinetic energy dissipation rate and heat transfer characteristics in the impinging region have been predicted by finite volume scheme for the various plate spacings.

Key Words-Confinement impinging jets; free turbulence; κ-ε turbulence model

1. INTRODUCTION

Impinging jets are used in a variety of heat and mass transfer applications including the glass and metal industries for cooling, in the paper and textile industries for drying, and thermal control of high heat flux electronics. The heat and mass transfer characteristics beneath an impinging jet depend largely on the nature of the flow field. For this reason it is essential to understand the flow characteristics for the investigation of the associated transport properties.

For direct contact drying of extended surface materials, impinging jets give substantially higher drying rates relative to parallel flows. Additionally, impinging jets have the potential for fine control of local drying rates by adjusting the geometry and/or local flow rate. This capability is particularly important in the drying of materials for which uniformity is a key requirement of product quality, such as in the drying of paper. Design of industrial impingement drying systems therefore involves an impressive number of alternatives and parameters, for which a complete understanding and documentation would require long programs of experimentation. The impingement drying of paper was investigated experimentally in pilot scale [1]. Looney and Walsh [2] used the κ-ε model for the prediction of heat transfer in the impingement region and indicated that a more complex turbulence model does not necessary improve the predictions. The κ-ε model thus retains a reasonable combination of economy and accuracy even for the complex configuration of impingement flow.

Polat et al. [3] investigated the modelling of convective heat transfer for impingement drying. Using the κ-ε model and the numerical solution was done by upwind finite difference scheme in their study.

Seyedein et al. [4] presented results of numerical simulation of two-dimensional flow field and heat transfer due to laminar heated multiple slot jets discharging normally into a converging confined channel. They employed a control volume-based finite difference method to solve the governing mass, momentum and energy equations.
Abe et al. [5] have developed a new turbulence model for flow field, which is modified from the latest low-Reynolds-number κ-ε model, to calculate complex turbulent flows with separation and heat transfer.

Cho and Goldstein [6] presented a revised form of low-Reynoldsnumber κ-ε turbulence model that aptly describes recirculating flows. It was applied to two-dimensional channel flows, flow over a backward facing step, and flow over a forward facing to calculate flow fields and surface heat or mass transfer rates. Considerable experimental and theoretical works on turbulent flows have been reported in the literature[7-9].

Using PHOENICS, Jambunathan et al. [10] and Yavuz [11] investigated the flow field between two horizontal stationary surfaces arising from the turbulent incompressible jet issuing from the upper and impinging normally on the lower surface. The velocity, pressure and shear stress distributions in the impinging region were predicted for a parabolic and a flat velocity profile with various plate spacings and Reynolds numbers.

Kopaç[12] evaluated the turbulence models for the air jet. Kopaç[13] used the κ-ε turbulence model for the numerical simulation of a gaseous fueled(methane) combustor. Park and Sung[14] developed a near-wall turbulence model and applied to heat and fluid flows for an impinging jet flow.

The objective of this study is to predict the flow and heat transfer characteristics in turbulence plane impinging jet partially confined by parallel surfaces using the two-equation turbulence model, κ-ε. To determine flow fields and heat transfer characteristics the PHOENICS package programme were used. Predictions were tested for close nozzle-to-surface spacings, $H=z_{max}/W$, in the range 1 to 4, for jets discharging from nozzles located in a confinement hood.

2. GOVERNING EQUATIONS ON THE PLANE IMPINGEMENT JET

A general form for the governing equations including the equation of continuity is:

$$\frac{\partial}{\partial y}(\rho v \phi) + \frac{\partial}{\partial z}(\rho w \phi) = \frac{\partial}{\partial y}\left(\Gamma_\phi \frac{\partial \phi}{\partial y}\right) + \frac{\partial}{\partial z}\left(\Gamma_\phi \frac{\partial \phi}{\partial z}\right) + S_\phi \qquad (1)$$

In order to express the governing equations of a particular variable in the above generalized form, the terms other than those in the form of "convection" and "diffusion" terms are collected in the source term, S_ϕ . The terms Γ_ϕ and S_ϕ are shown in Table 1. As turbulent viscosity, μ_t, is determined by flow conditions, it must be modeled in terms of measurable flow quantities. This is done using the two equation κ-ε turbulence model of Jones and Launder[15]. In the κ-ε model, μ_t is related to the turbulence kinetic energy and to the dissipation of turbulent kinetic energy, κ and ε, as

$$\mu_t = C_\mu \rho \frac{\kappa^2}{\varepsilon} \tag{2}$$

The transport equations for κ and ε are summarized in Table 1.

The equation of continuity

$$\frac{\partial}{\partial y}(\rho v) + \frac{\partial}{\partial z}(\rho w) = 0 \tag{3}$$

y-momentum

$$\frac{\partial}{\partial y}\left(\rho v^2\right) + \frac{\partial}{\partial z}(\rho w v) = \frac{\partial}{\partial y}\left(\mu_{eff}\frac{\partial v}{\partial y}\right) + \frac{\partial}{\partial z}\left(\mu_{eff}\frac{\partial v}{\partial z}\right) - \frac{\partial P}{\partial y} + \frac{\partial}{\partial y}\left(\mu_{eff}\frac{\partial v}{\partial y}\right) + \frac{\partial}{\partial z}\left(\mu_{eff}\frac{\partial w}{\partial y}\right) \tag{4}$$

z-momentum

$$\frac{\partial}{\partial y}(\rho v w) + \frac{\partial}{\partial z}\left(\rho w^2\right) = \frac{\partial}{\partial y}\left(\mu_{eff}\frac{\partial w}{\partial y}\right) + \frac{\partial}{\partial z}\left(\mu_{eff}\frac{\partial w}{\partial z}\right) - \frac{\partial P}{\partial z} + \frac{\partial}{\partial y}\left(\mu_{eff}\frac{\partial v}{\partial z}\right) + \frac{\partial}{\partial z}\left(\mu_{eff}\frac{\partial w}{\partial z}\right) \tag{5}$$

The energy equation ($\bar{h} = \frac{h - h_{imp}}{h_{con} - h_{imp}}$)

$$\frac{\partial}{\partial y}(\rho v \bar{h}) + \frac{\partial}{\partial z}(\rho w \bar{h}) = \frac{\partial}{\partial y}\left(\left(\frac{\mu_\ell}{\sigma_\ell} + \frac{\mu_t}{\sigma_t}\right)\frac{\partial \bar{h}}{\partial y}\right) + \frac{\partial}{\partial z}\left(\left(\frac{\mu_\ell}{\sigma_\ell} + \frac{\mu_t}{\sigma_t}\right)\frac{\partial \bar{h}}{\partial z}\right) \tag{6}$$

κ and ε are determined from Rubel [16] ;

Turbulent kinetic energy equation;

$$\frac{\partial}{\partial y}(\rho v \kappa) + \frac{\partial}{\partial z}(\rho w \kappa) = \frac{\partial}{\partial y}\left(\left(\mu_\ell + \frac{\mu_t}{\sigma_\kappa}\right)\frac{\partial \kappa}{\partial y}\right) + \frac{\partial}{\partial z}\left(\left(\mu_\ell + \frac{\mu_t}{\sigma_\kappa}\right)\frac{\partial \kappa}{\partial z}\right) + G - \rho\varepsilon \tag{7}$$

Turbulent kinetic energy dissipation rate equation;

$$\frac{\partial}{\partial y}(\rho v\varepsilon)+\frac{\partial}{\partial z}(\rho w\varepsilon)=\frac{\partial}{\partial y}\left(\left(\mu_\ell+\frac{\mu_t}{\sigma_\varepsilon}\right)\frac{\partial \varepsilon}{\partial y}\right)+\frac{\partial}{\partial z}\left(\left(\mu_\ell+\frac{\mu_t}{\sigma_\varepsilon}\right)\frac{\partial \varepsilon}{\partial z}\right)+C_1\frac{\varepsilon}{\kappa}G-C_2\rho\frac{\varepsilon^2}{\kappa} \quad (8)$$

The numerical procedure allows solutions of the Navier-Stokes and energy equations in conjuction with the two-equation turbulence model, κ-ε. The sets of equations, incorporating the Boussinesq turbulent viscosity concept, which describe the mean velocity, pressure and temperature fields for steady axiymmetric turbulent flow considering Eq. (1) and Table 1 are given as follows:

Table 1. Summary of the basic equations

Equation	ϕ	Γ_ϕ	S_ϕ
Continuity	1	0	0
y - momentum	v	μ_{eff}	$-\frac{\partial P}{\partial y}+\frac{\partial}{\partial y}\left(\mu_{eff}\frac{\partial v}{\partial y}\right)+\frac{\partial}{\partial z}\left(\mu_{eff}\frac{\partial w}{\partial y}\right)$
z - momentum	w	μ_{eff}	$-\frac{\partial P}{\partial z}+\frac{\partial}{\partial y}\left(\mu_{eff}\frac{\partial v}{\partial z}\right)+\frac{\partial}{\partial z}\left(\mu_{eff}\frac{\partial w}{\partial z}\right)$
Energy	h	$\frac{\mu_\ell}{\sigma_\ell}+\frac{\mu_t}{\sigma_t}$	0
Turbulent energy	κ	$\mu_\ell+\frac{\mu_t}{\sigma_\kappa}$	$G-\rho\varepsilon$
energy dissipation	ε	$\mu_\ell+\frac{\mu_t}{\sigma_\varepsilon}$	$C_1\frac{\varepsilon}{\kappa}G-C_2\rho\frac{\varepsilon^2}{\kappa}$

Where

$$G=\mu_t\left\{\left(\frac{\partial v}{\partial z}+\frac{\partial w}{\partial y}\right)^2+2\left[\left(\frac{\partial v}{\partial y}\right)^2+\left(\frac{\partial w}{\partial z}\right)^2\right]\right\};\quad \mu_{eff}=\mu_\ell+\mu_t$$

$C_\mu=0.09$; $C_1=1.43$; $C_2=1.92$; $\sigma_\kappa=1.0$; $\sigma_\varepsilon=1.3$; $\sigma_t=0.9$

Boundary Conditions:

For the flow configuration used, Fig. 1, the boundary conditions are as follows.

Nozzle exit: Uniform profiles for the jet across the slot nozzle exit are specified for velocity, w_j, axial turbulence intensity, I_j=1%, and nondimensional entalpy, $\bar{h}_j$=1. These w_j and I_j conditions are realistic for the ASME standart elliptically contoured entry nozzle. The boundary conditions for v, κ and ε are:

$$v_j = 0; \quad \kappa_j = I_j^2 w_j^2; \quad \varepsilon_j = C_\mu \, \kappa_j^{3/2} / (0.03\frac{W}{2})$$

Symmetry Axis: $$v = \frac{\partial w}{\partial y} = \frac{\partial \kappa}{\partial y} = \frac{\partial \bar{h}}{\partial y} = \frac{\partial \varepsilon}{\partial y} = 0$$

At the Impingement and Confinement Surfaces: The following conditions were specified at the confinement and impingement surfaces, respectively:

$$w = 0; \; v = 0; \; \bar{h}_{con} = 1; \; \bar{h}_{imp} = 0; \quad \kappa = \varepsilon = 0$$

Outflow: $$w = \frac{\partial v}{\partial y} = \frac{\partial \kappa}{\partial y} = \frac{\partial \bar{h}}{\partial y} = \frac{\partial \varepsilon}{\partial y} = 0$$

To apply these outflow boundary conditions this boundary should be placed at a sufficient distance from the jet axis to avoid inflow across part of this boundary.

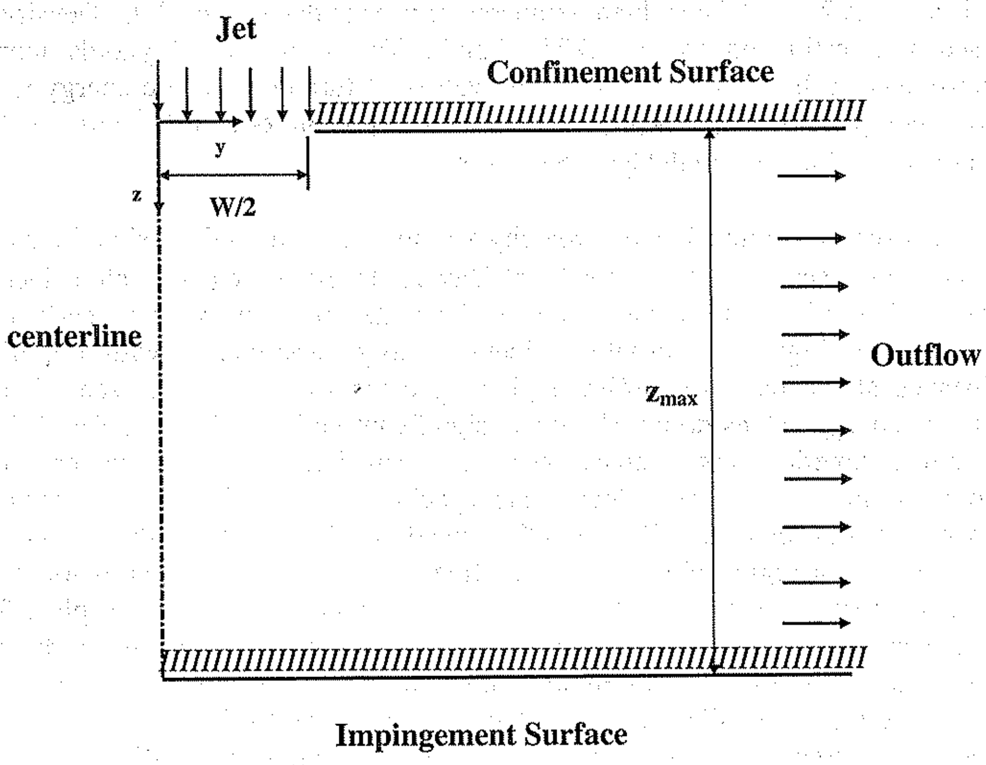

Figure 1. Confined impinging plane jet flow configuration.

3. NUMERICAL PROCEDURE

The PHOENICS code developed by Spalding[17] was modified for use in the present work.

Grid Layout:

A rectangular coordinate system was used to discretize the flow field. In order to achieve efficiency in terms of computational time as well as accuracy in regions of steep and mild gradients, a combination of uniform and non-uniform grid size appropriate to the flow field was used. In the y-direction, from the jet symmetry line to the nozzle corner, a uniform grid spacing was used so that the nozzle wall coincides with a control volume boundary. Downstream of the nozzle an expanding y-direction grid layout (factor 1.05) was adopted. In the z-direction, i.e. from confinement to impingement surface, the grid layout was uniform. In the runs the number of grid nodes was 5÷20(1.05) in the y-direction and 25(uniform) in the z-direction.

4. RESULTS AND DISCUSSION

In this study, the values of velocity, nondimensional enthalpy, turbulent kinematic viscosity, turbulent kinetic energy and turbulent kinetic energy dissipation rate were calculated numerically for four different plate spacings. The temperature of air used in this study is 20 °C. The ambient temperature is considered to be 0 °C. Density of the air used was estimated to be 1.2045 kgm^{-3}. The values of Reynolds number were considered to be $1x10^4$ and $3x10^4$.The values of turbulent kinetic energy in this study were compared with the results of Polat et al.[3] when Re = $3x10^4$ and H = 2.6. In this study κ-ε turbulence model have been used.

As seen in Figure 2, axial velocity variation with non-dimensional distance above plate are consistent with the results of Yavuz[11]. Axial velocity values increase up to the half length of the distance above the plate and then remain nearly constant at Y=0.03. In Figure 3, turbulent kinetic energy variation, Z with non-dimensional distance above plate for different plate spacings are given. It is seen that turbulent kinetic energy values do not show any significant variation at H=1. For H=2 and H=4, turbulent kinetic energy values decrease, when distance of impingement plate from confined plate increases. When plate spacing value(H) increases, turbulent kinetic energy values increase. On the other hand, as H increases, these values reach a minimum at a region closer to the confined plate. In Figure 4, variation of turbulent kinetic energy dissipation along the non-dimensional distance above plate for H=1, 2 and 4 are given. These variations show a similar trend as with the turbulent kinetic energy shown in Figure 3. In Figure 5, predicted non-dimensional enthalpy values along the non-dimensional distance above the plate are given for H=1, 2 and 4. These values show an increase from the impingement plate through the confined plate and, they converge to each other approaching to the confined plate. Turbulent kinetic energy variations along the non-dimensional distance from the nozzle centerline are given in Figure 6. As seen from this plot turbulent kinetic energy passes through a maximum at the middle and then slow a decrease, for H= 1. As H increases, maximum values shift to lower values and the variation in turbulent kinetic energy values remains essentialy constant. As plate spacing values increase, maximum points approach to nozzle centerline. For each of three plate spacings, the results are the same at Y=0.33. As H increases, the values before this point increase. In Figure 7, turbulent kinetic energy variation of this study is compared with Polat et al. [3]. The results of this study are seen to be consisted with Polat et al. [3].

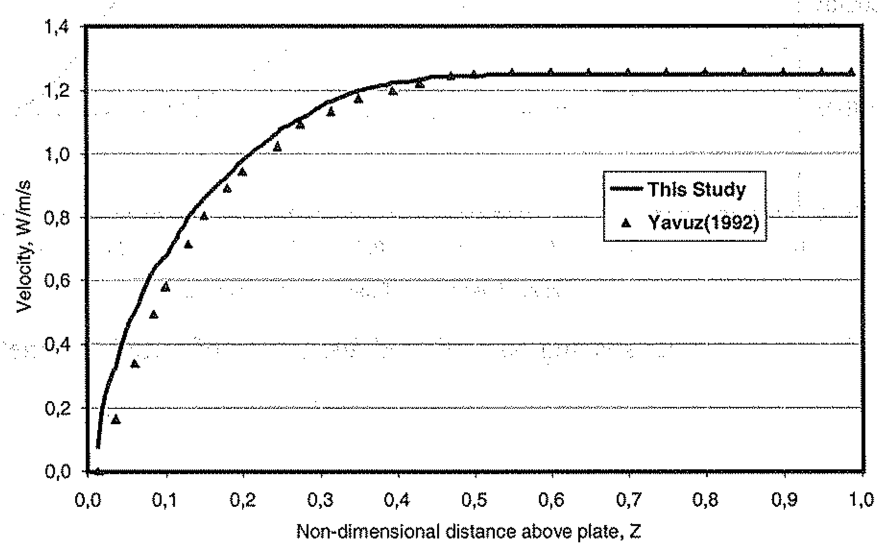

Figure 2. Comparison of axial velocities along the symmetry axis when H = 2 and Re=10000, $Y(y/y_{max})$=0.03

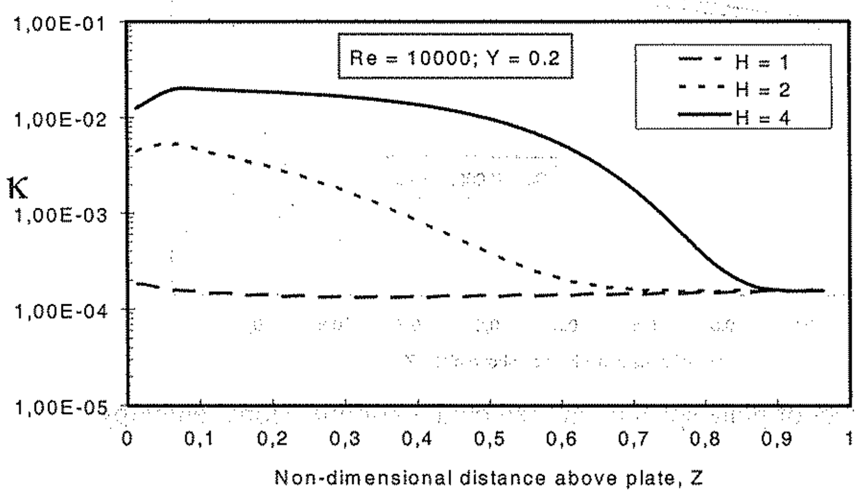

Figure 3. Effect of plate spacing on predicted turbulent kinetic energy

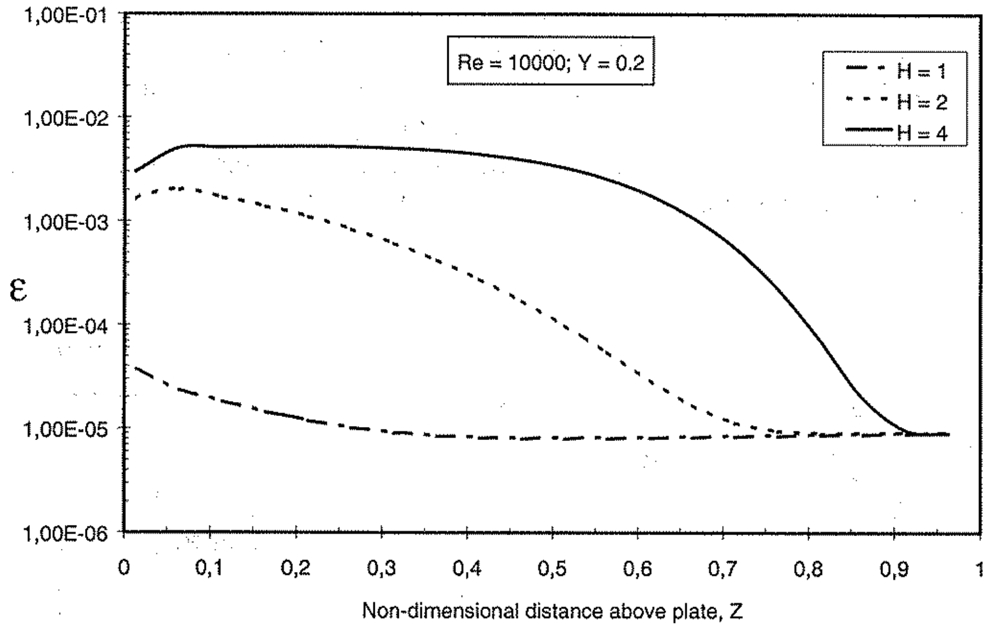

Figure 4. Effect of plate spacing on predicted dissipation of turbulent kinetic energy

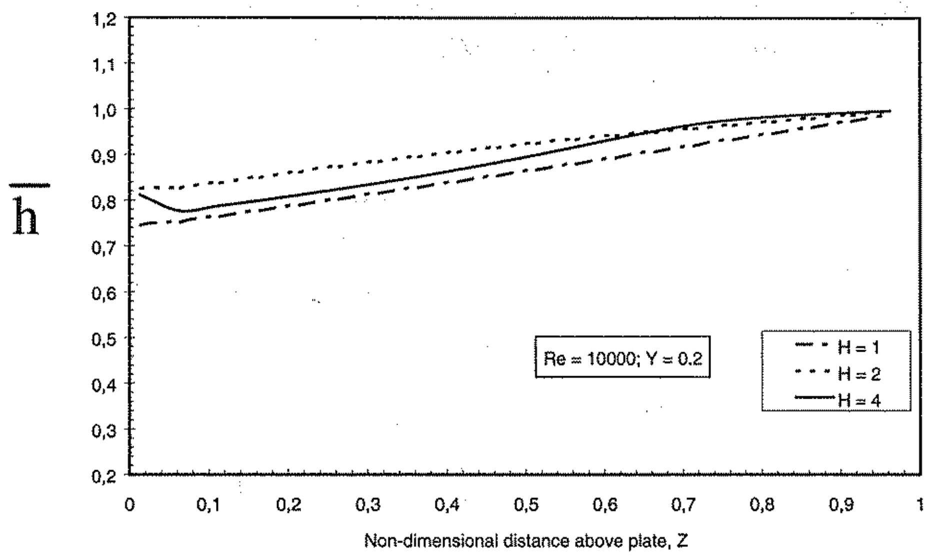

Figure 5. Effect of plate spacing on predicted non-dimensional enthalpy

REFERENCES

1. B. W. Burgess, W. Seto, E. Koller and I. T. Pye, The paper dryer process, *Part II, Mill trials, Pulp and Paper Mag. Can.*, **73**, 323-331, 1972.
2. M. K. Looney and J. J. Walsh, Mean flow and turbulent characteristics of free and impinging jet flows, *J. Fluid Mech.*, **147**, 397-429, 1984.
3. S. Polat, A.S. Mujumdar, A.R.P. van Heinigen and W. J. M. Douglas, Effect of near-wall modelling on prediction of impingement heat transfer, *J. Dry. Tec.*, **8**, 705-730, 1990.
4. S. H. Seyedein, M. Hasan and A. S. Mujumdar, Laminar flow and heat transfer from multiple impinging slot jets with an inclined confinement surface, *Int. J. Heat Mass Tran sfer*, **37**, 1867-1875, 1994.
5. K. Abe and T. Kondoh, A new turbulence model for predicting fluid flow and heat transfer in separating and reattaching flows: -1. Flow field calculations, *Int. J. Heat Mass Transfer*, **37**, 139-151, 1994.
6. H. H. Cho and R. J. Goldstein, An improved low-Reynolds-number κ-ε turbulence for recirculating flows, *Int. J. Heat Mass Transfer*, **37**, 1495-1508, 1994.
7. T. Karasu, O. Kural, N. Eğrican, Ö. E. Ataer, O. Borat and O. Özcan, Computer Simulation of Turbulent Flow Over Backward-Facing Steps, *Fourth Turkish National Combustion Symposium*, Proceedings, 370-379, Bursa, 19-21 July 1995.
8. T. Karasu, Numerical Prediction of Turbulent Recirculating Flow Through Axisymmetric Sudden Expansions, *10th International Conference on Numerical Methods for Laminar and Turbulent Flow*, Proceedings, 10, Swansea, U.K., 21st – 25th July 1997.
9. T. Karasu and D. B. Spalding, Prediction of Turbulent Swirling Flows in Annuli, *J. of the Faculties of Engineering of Uludağ University*, **1**, 21-42, 1984.
10. K. Jambunathan, S. Kapasi, B. L. Button and J. A. Bland, Numerical study of flow field of confined laminar jet impingement, *Third Int. PHOENICS User Conference,* Dubrouvnik, Yugoslavia, 28 August-1 Sept., 1989.
11. T. Yavuz, Effects of Turbulence Modellings on Prediction of Flow and Heat Transfer Characteristics for Confined Jet Impingement, *Tr. J. of Engineering and Environmental Sciences*, **16**, 177-192, 1992.
12. M. Kopaç, Hava Jet Akımı için Türbülans Modellerinin Değerlendirilmesi, *11. Ulusal Isı Bilimi ve Tekniği Kongresi,* **2,** 785-794, Edirne, 17-19 Eylül 1997.
13. M. Kopaç and T. Kopaç, Numerical simulation of a gaseous fueled(methane) combustor, *Mathematical & Computational Applications,* **2(3),** 101-118, 1997.
14. T. S. Park and H. J. Sung, Development of a near-wall turbulence model and application to jet impingement heat transfer, *Int. J. Heat and Fluid Flow,* **22(1),** 10-18, 2001.
15. W. P. Jones and B. E. Launder, The Calculation of low-Reynoldsnumber phenomena with a two-equation model of turbulence, *Int. J. Heat and Mass Transfer*, **16,** 1119-1130, 1973.
16. A. Rubel, Computations of the oblique impingement of round jets upon a plane wall *AIAA J.,* **19**, 863-871, 1981.
17. D. B. Spalding, PHOENICS, CHAM Ltd., London, 1980.